

Model-Free Power-Spectral-Density Estimation for Low-Light-Level CMOS Imaging Sensors

Radu Ispasoiu, José R. Camara, and Boyd A. Fowler

Fairchild Imaging, 1801 McCarthy Blvd., Milpitas, CA 95035 USA

Abstract—We report on a method to estimate the noise power spectral density (PSD) of a CMOS image sensor (CIS), without any prior analytical assumptions. The method is based on the swept time operation of the correlated double sampling (CDS) output of a low-light-level CIS. We illustrate the method’s applicability through a direct frequency domain analysis of noise contributions to the sensor performance. The method is demonstrated to reveal useful frequency domain information about the PSD of pixels showing distinct noise behavior. We also provide results validating the frequency domain calibration of the method.

I. INTRODUCTION

RECENT advances in CMOS image sensors (CIS) have demonstrated devices with readout noise less than $2e$ -RMS [1,2]. In order to continually improve the read noise in CIS, tradeoffs between pixel level and column level noise contributions need to be accurately measured. This includes estimating the power spectral density of the noise sources and subsequently understanding the nature of the noise sources from their characteristic signatures in the frequency domain [3]. In this paper we develop a method to estimate the power spectral density (PSD) of both pixel and column level circuitry using correlated double sampled (CDS) data from the output of a typical CIS. Specifically, we report on a model-free PSD estimation method that makes no assumptions about the noise sources in the readout path before CDS.

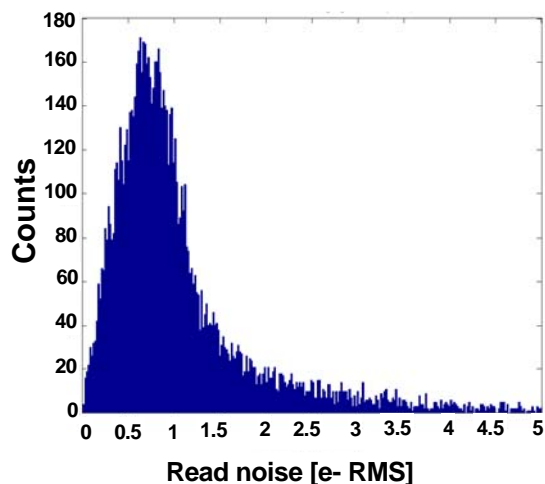


Figure 1. High-gain channel read noise distribution

The method is based on sweeping the time delay between CDS noise samples. The subsequent autocorrelation estimation and Fourier transformation of the data leads to a full frequency domain representation of the noise. We developed this method because direct time domain sampling of the sensor output and subsequent summation and Fourier transformation leads to complicated merging of the intermediate frequency domain data, i.e. frequency domain data generated using different CDS sampling periods.

This method was developed to characterize the origins of noise from various percentiles of a CIS read noise histogram. Such a histogram is shown in Figure 1 as recorded for a CIS described in detail in [1, 2]. The ultimate goal is to obtain more information about the various noise components in low light level CIS, and use this information to reduce the median read noise and standard deviation of the noise distribution.

The paper is structured as follows: in Section II we provide a description of the mathematical formalism underlying the method; Section III analyzes the method capabilities and limitations; in Section IV we illustrate the application of this method using two types of pixels from opposite ends of the noise histogram shown in Figure 1. In addition, we show that the frequency domain mapping is accurate. Finally Section V concludes the paper.

II. METHOD DESCRIPTION

A block diagram of a typical high gain readout path from a CIS pixel is shown in Figure 2. The signal path from the pixel flows through a high gain amplifier that is low-pass filtered (LPF) at a cutoff frequency f_0 and then subjected to correlated –double sampling (CDS) onto two capacitors. The output differential signal $Z(t)$ is the CDS output proportional to the charge collected at the pixel and containing the additive output noise component $\varepsilon(t)$. Note that $B(t)$ represents the input signal as a function of time, $N(t)$ is the input referred sensor noise (such as $1/f$, RTS, white-noise), and $X(t)$ represents the pre-CDS signal. The signal path before the sampling is measured in voltage while after the sampling it is expressed in digital numbers (DN). The signal at the CDS input is expressed as the convolution – represented by the \otimes symbol:

$$X(t) = [B(t) + N(t)] \otimes h(t), \quad (1)$$

where $h(t)$ is the temporal transfer function of the column amplifier and low-pass filter (LPF).

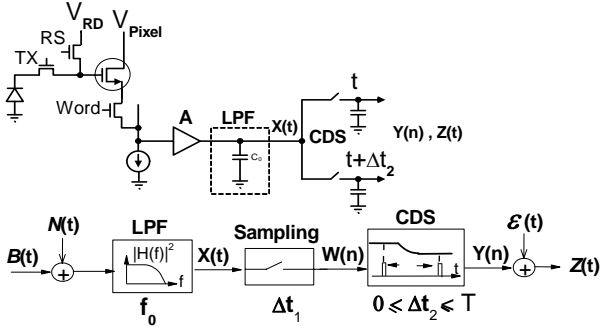


Figure 2. Pixel level readout path schematic and signal flow diagram.

The sensor output signal resulting from sampling with period Δt reads as:

$$\begin{aligned} Z(t) &= X(t + \Delta t) - X(t) = \\ &= [B(t + \Delta t) - B(t) + N(t + \Delta t) - N(t)] \otimes h(t) \end{aligned} \quad (2)$$

The output signal noise can be used to infer information about noise sources at the sensor input. The traditional approach [3, 4] for measuring sensor noise involves collecting long sequences of data under dark conditions. This data is then processed to calculate the variance of the sensor noise. Although this method gives sensor noise information, it does not lead to an estimate of the noise PSD.

Here we report on a different approach that allows us to estimate the power spectral density $S_N(f)$ of $N(t)$, by sweeping the time delay Δt_2 between correlated samples, from zero to a fixed value T . This can be demonstrated by first finding the variance of the output signal $Z(t)$ as a function of its inputs:

$$\begin{aligned} \sigma_Z^2(\Delta t_2) &= E[Z^2(t)] = \\ &= E[X^2(t + \Delta t_2) - 2X(t)X(t + \Delta t_2) + X^2(t)] = \\ &= 2[R_X(0) - R_X(\Delta t_2)], \end{aligned} \quad (4)$$

where R_X is the autocorrelation function of $X(t)$. $S_X(f)$, the PSD of $X(t)$, is given by the Fourier transform of $R_X(\Delta t)$ i.e.

$$S_X(f) = \int_{-\infty}^{\infty} R_X(\Delta t) e^{-j2\pi f \Delta t} d(\Delta t). \quad (5)$$

Using equations (4) and (5)

$$S_X(f) = \int_{-\infty}^{\infty} \left[R_X(0) - \frac{\sigma_Y^2(\Delta t)}{2} \right] e^{-j2\pi f \Delta t} d(\Delta t). \quad (6)$$

Note that we have assumed that $Z(t)$ is a random variable with zero mean and finite variance, and that $\lim_{\Delta t_1 \rightarrow \infty} R_X(\Delta t_1) \rightarrow 0$. Under dark conditions the PSD of $N(t)$ is given by:

$$S_N(f) = S_X(f) / |H_{LPF}(f)|^2, \quad (7)$$

where $|H_{LPF}(f)|^2 = A^2 / \left[1 + \left(\frac{f}{f_0} \right)^2 \right]$ is the transfer

function of column amplifier and LPF (where A is amplifier gain coefficient).

Assuming that $X(t)$ is a zero mean random process with finite variance ($E[X^2(t)] < \infty$), implies that the autocorrelation of $X(t)$ tends to zero at infinite sampling times, i.e. $\lim_{T \rightarrow \infty} R_X(T) \rightarrow 0$. Therefore the input referred power spectral density is:

$$S_N(f) = \frac{1}{2|H_{LPF}(f)|^2} \int_{-\infty}^{\infty} \left[\lim_{\tau \rightarrow \infty} \sigma_Z^2(\tau) - \sigma_Z^2(\tau) \right] e^{-j2\pi f \tau} d\tau \quad (8)$$

Equation (8) indicates that $S_N(f)$ can be estimated based on the measurement of $Z(t)$ versus the CDS sampling period variation when the sensor is operated under dark conditions.

III. METHOD ANALYSIS

In order to demonstrate the validity of the method we used a frequency domain $1/f$ noise model based on a superposition of low-pass filtered Gaussian white noise sources with the low-pass filters in an exponential progression [6]. The algorithm yielded the noise PSD $S_N(f)$ from which the variance was calculated as an integral over the entire bandwidth:

$$\sigma_N^2 = \int_{-\infty}^{\infty} S_N(f) df \quad (9)$$

The noise autocorrelation function R_X was calculated based on the formalism of equation (4). Figure 3 shows the modeled noise variance and autocorrelation. Based on the autocorrelation result, the noise PSD was estimated according

to equation (8) and it was in excellent agreement with the modeled PSD shown in Figure 4.

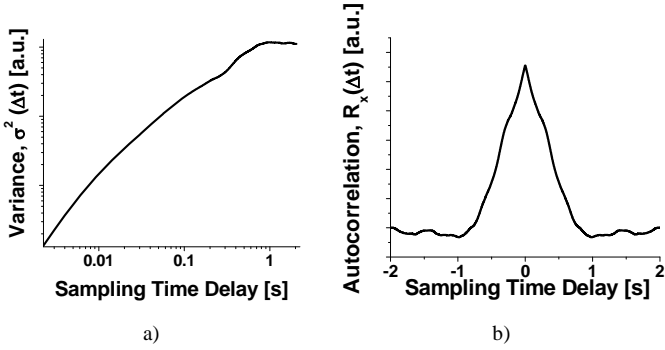


Figure 3. a) the $1/f$ noise variance as a function of Δt ; b) the autocorrelation of the $1/f$ noise signal.

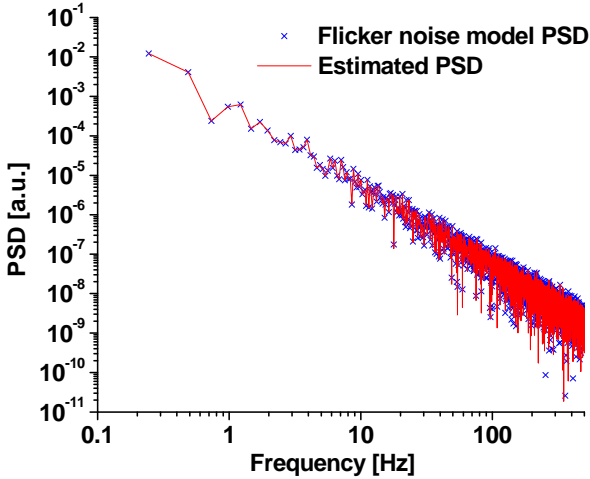


Figure 4. Comparison between modeled $1/f$ noise PSD (dots) and the estimated PSD based on processing the variance data (figure 3.a) according to equation (8).

The PSD recovery error is characterized by two factors: the frequency axis uncertainty governed by the minimum CDS time sampling interval, and the signal axis uncertainty governed by the number of statistical samples taken for the pixel signal at each CDS sampling interval.

In that respect, if pixel signal $Z(t)$ is measured m times at a given sampling time, and the average signal for all the m measurements taken is $\overline{Z(t)}$, an unbiased estimator for the data population variance [7] is

$$\hat{\sigma}_Z^2 = \frac{1}{m-1} \sum_{j=1}^m [Z_j(t) - \overline{Z(t)}]^2. \quad (10)$$

If we assume that $Z(t)$ is zero mean Gaussian random process with finite variance then the variance of $\hat{\sigma}_Z^2$ is:

$$\sigma_{\hat{\sigma}_Z^2}^2 = \frac{2\sigma_Z^4}{m-1}. \quad (11)$$

Equation (11) comprises the quantitative dimension of the intuitively expected fact that the noise measurement error, and consequently the accuracy of the PSD estimator increases with the number of dark frames m . Using (11) it can be shown that the variance of

$$\hat{R}_X(\Delta t) = \frac{1}{2} (\hat{\sigma}_Z^2(T) - \hat{\sigma}_Z^2(\Delta t)), \quad (12)$$

is

$$\sigma_{R_X}^2 = \frac{(\sigma_Z^4(T) + \sigma_Z^4(\Delta t))}{2(m-1)}. \quad (13)$$

$S_N(f)$ is estimated using

$$\hat{S}_N(f) = \frac{1}{A^2} \sum_{i=-n}^n \hat{R}_X(Ti/n) e^{-j2\pi f Ti/n}. \quad (15)$$

Note that the LPF in the column amplifier is used for anti-aliasing and therefore is not considered in equation (15). Although beyond the scope of this paper the bias and variance of $\hat{S}_N(f)$ can be derived using methods similar to those described in [8]. The signal-to-noise-ratio of the resulting PSD is low and for successful application in experimental conditions averaging over an optimum number of frequency bins is necessary.

IV. EXPERIMENTAL DATA AND DISCUSSION

Most of the noise analysis techniques employed for image sensors rely on *a priori* temporal modeling assumptions in order to infer frequency domain information. The method described here is able to provide a direct frequency domain analysis of the CIS noise components.

The CIS used for investigating our method was a device with low readout noise of 0.8e- RMS [2]. The CDS was operated in swept mode while driven by a 30MHz clock - such that the fastest sampling interval was 33.333 ns. The characteristic low-pass filtering frequency was $f_0 = 556\text{kHz}$. Figure 5 shows the CDS output variance signals measured for two extremely different pixels from the CIS. Equation (8) was applied for processing the variance data and the estimated PSDs for the two pixels are displayed in Figure 6. The displayed frequency bandwidth is limited here to 1MHz where most of the useful information can be found. From the

estimated PSD results in Figure 6 it can be inferred that both pixels exhibit dominant $1/f$ type noise contributions with additional white noise component for Pixel 1 at lower frequencies. Future work will be focused on demonstrating the ability of this method to serve as an investigative tool correlating fabrication process details with noise contributions identified in various pixel types.

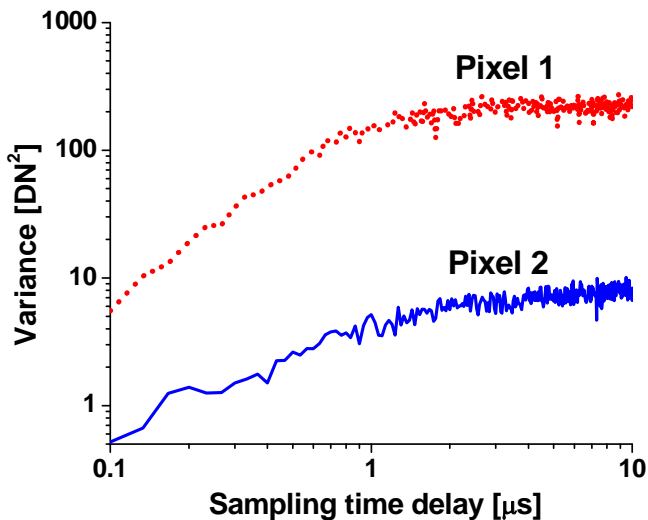


Figure 5. The CDS output variance for two distinctively different CIS pixels.

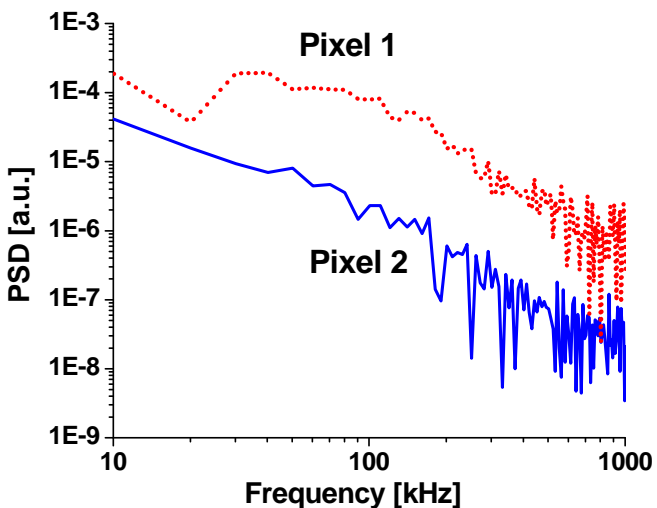


Figure 6. The noise PSD recovered by our method for the two pixels with variance shown in Figure 4. CDS output variance for two distinctively different CIS pixels.

To calibrate the frequency domain accuracy of the method we injected different sinusoidal tones into the CIS signal path to verify if the dominant spectral component is detected in the

estimated PSD. Shown in Figure 7 are the resulting clearly recovered peaks from 50 and 100kHz tone injection. The spectral accuracy is limited by the sampling delay itself.

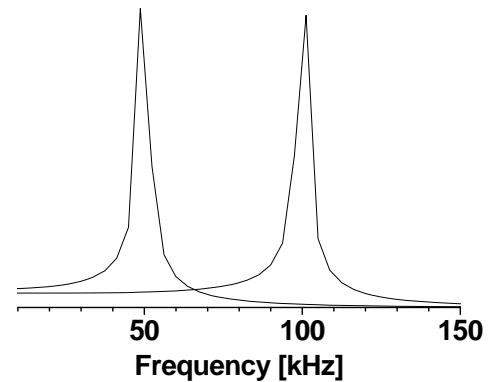


Figure 7. Noise PSD recovered for two signals with distinct tone injection at 50kHz and 100kHz respectively.

V. CONCLUSION

A model-free method for estimating the PSD of CIS operated with variable CDS sampling time is proposed. The method was validated against a $1/f$ noise source model as well as against single sinusoidal tone injection into the CIS signal path, giving excellent results. The method was applied to estimating the PSD of low-light-level CIS pixels with distinct time-domain noise behavior. The resulting estimated PSD's for two such pixels provided unambiguous frequency domain indication of distinct noise components. By injecting single frequency tones at the pixel input we were able to verify the accuracy of the frequency mapping through this technique.

REFERENCES

- [1] B. Fowler, X. Liu, P. Vu, "CMOS image sensors – past, present and future", Proceedings ICIS 2006 – International Congress of Imaging Science (2006) pp.134-141.
- [2] B. Fowler, C. Liu, S. Mims, J. Balicki, W. Li, H. Do, P. Vu, "Low-light-level CMOS image sensor for digitally fused night vision systems", SPIE vol. 7298 "Defense Security and Sensing" (2009).
- [3] S. Mims, B. Fowler, B. Frymire, "1/f noise measurement in CMOS image sensors", Proceedings 2005 IEEE Workshop on CCD and AIS.
- [4] N. Kawai, S. Kawahito, "Effectiveness of a correlated multiple sampling differential averager for reducing 1/f noise", IEICE Electronics Express, vol.2, no.13, pp.379-383 (2005).
- [5] G. R. Hopkinson, D. H. Lumb, "Noise reduction techniques for CCD image sensors", J. Phys. E: Sci. Instrum., vol. 15, pp.1212-1222 (1982).
- [6] A. van der Ziel, "Noise in solid state devices and electronic circuits", Wiley, New York (1986).
- [7] A. Papoulis, "Probability, Random Variables and Stochastic Processes", McGraw-Hill, New York (1984).
- [8] K. Shanmugan and A. Breipohl, "Random Signals Detection, Estimation and Data Analysis", Wiley, New York (1988).